scientific reports

Check for updates

OPEN

Serum MicroRNA signatures associated with hypertrophic callus formation in polytrauma patients with traumatic brain injury

Thomas Lettner[1,2,10], Florian Dussing[3,4,10], Renate Gehwolf[1,2], Christian Deininger[1,4], Amelie Deluca[1], Verena Wally[5,6], Valeska Hofmann[7,8], Matthias Hackl[2,9], Andreas Traweger[1,2]✉ & Florian Wichlas[4,8]

Long-bone fractures occasionally develop excessive callus formation in the presence of traumatic brain injury, a clinically relevant but poorly understood injury response. Although this phenomenon is known for decades, the causal factors are still underexplored, and no systemic biomarkers are currently available to predict the exuberant bone-mass-formation at an early timepoint after injury. In this study, we used small-RNA-seq, bioinformatic analyses, and in vitro assays to identify a set of micro-RNAs in sera of hypertrophic callus patients that could serve as potential biomarkers. The identified miRNAs are highly expressed in the human brain, particularly in the pituitary gland, and have been shown to regulate mRNA targets implicated in osteogenic processes.

Keywords Long-bone fracture, Traumatic-brain-injury, Hypertrophic-callus, miRNA, DLK1-DIO3, Pituitary gland

It is a common observation among orthopedic trauma surgeons that fractures occasionally heal with increased callus-formation and/or accelerated fracture-union when patients suffer a concomitant traumatic brain injury (TBI)[1,2]. Although clinical reports of this phenomenon reach back to the 1960s[3], knowledge about the causal factors remains largely elusive. Several hypotheses have been proposed to explain the phenomenon[4]. However, to the best of our knowledge, aside from studies in murine models[5–7], it has not yet been systematically investigated in humans on a molecular level.

Any factor that triggers TBI-associated, excessive callus-formation potentially originates from the brain and is being released to the blood stream during or in the wake of brain injury. Potential biomarkers have been investigated in animal and human studies that analyzed humoral components in fracture healing in combination with TBI. Neither of these studies identified the causal factors of accelerated or increased callus-formation in the context of TBI unambiguously, and none of the analyzed humoral components proved suitable as biomarkers to predict the risk of acquiring a hypertrophic callus[8–11].

Among the candidate humoral components of interest, micro-RNAs (miRNAs) have garnered significant attention over the last two decades, both broadly and specifically as biomarkers in bone diseases[12,13]. miRNAs are short (~ 22nt), single stranded oligonucleotides that primarily bind to the 3'-UTR of protein-coding mRNAs, resulting in downregulation or complete repression of target gene expression on the protein level[14]. Although several studies were able to assign certain miRNA signatures individually to either fracture healing[15–17] or TBI[18–20], respectively, the combined occurrence of miRNAs in fracture healing, TBI and hypertrophic callus-formation has not been investigated in human patients.

[1]Institute of Tendon and Bone Regeneration, Paracelsus Medical University, Salzburg, Austria. [2]Austrian Cluster for Tissue Regeneration, Vienna, Austria. [3]Department of Orthopedics, General Hospital Oberndorf, Oberndorf, Austria. [4]Department of Orthopedics and Traumatology, University Hospital of the Paracelsus Medical University, Salzburg, Austria. [5]Department of Dermatology and Allergology, University Hospital of the Paracelsus Medical University, Salzburg, Austria. [6]EB House Austria, Research Program for Molecular Therapy of Genodermatoses, Department of Dermatology and Allergology, University Hospital of the Paracelsus Medical University, Salzburg, Austria. [7]Department of Orthopedic and Trauma Surgery, Karl-Olga-Krankenhaus, Stuttgart, Germany. [8]No Limit Surgery, Salzburg, Austria. [9]Department of Research and Development, TAmiRNA GmbH, Vienna, Austria. [10]Thomas Lettner and Florian Dussing contributed equally to this work. ✉email: andreas.traweger@pmu.ac.at

We hypothesized that serum levels of miRNAs differ between callus-patients vs. non-callus patients in the context of TBI. We therefore performed small-RNA-seq to identify miRNA markers in serum of bone-fracture-patients, TBI-patients, TBI-fracture-patients without hypertrophic callus and TBI-fracture-patients with hypertrophic callus formation. RNA-seq results were then analyzed bioinformatically and confirmed by in vitro experiments.

In this study, we show that patients with TBI and bone fractures, who develop a hypertrophic callus, express increased serum-levels of hsa-miR-127-3p, hsa-miR-376a-3p, hsa-miR-411-5p, hsa-miR-431-5p, hsa-miR-487b-3p, hsa-miR-543 and hsa-miR-654-5p. These miRNAs are all encoded on a parentally imprinted genomic cluster on human chromosome 14q32 (C14q32), also known as *DLK1-DIO3* cluster[21,22].

Investigation of tissue-specific gene expression data further showed that candidate C14q32 miRNAs are highly expressed in the human brain, particularly in the pituitary gland. In-silico analysis of miRNA target networks indicated that several of the identified candidate miRNAs are predicted to regulate transcripts encoding proteins implicated in neuronal signaling and bone homeostasis. In line with these predictions, we demonstrate that transfection of hBMSCs with a mimic of the candidate miRNA hsa-miR-543 results in a marked downregulation of RANKL (TNFSF11), a key regulator of osteoclast differentiation[23].

The set of candidate miRNAs identified in our study represents a potential link between brain- and bone biology. Notably, for the first time since the recognition of the heightened risk of abnormal bone healing, these miRNAs represent promising serological biomarkers to predict hypertrophic callus formation in patients who have sustained a concomitant traumatic brain injury.

Results

Approximately one third of included patients with TBI and fractures develop a hypertrophic callus

The present study included 31 patients grouped into four separate classes, according to the type of underlying injury: Fx, TBI, TBI + Fx, TBI + Fx + Call (Fig. 1A). One female patient was excluded due to pre-existing osteoporotic condition and several patients could not be included due to transfer to other hospitals shortly after their condition stabilized. Patient groups and injuries are shown in Figs. 1 and 2 and detailed demographics are presented in Table 1. Overall, patient age ranged from 16 to 80 years, of whom ten patients were female (32%) and 21 were male (68%). Thirteen patients had either isolated or multiple bone-fractures (Fx), nine patients suffered traumatic brain injuries (TBI) and nine patients had sustained TBI and fractures. All TBIs were classified as "severe" (GCS 3 to 8) according to the *Glasgow coma scale*[24] and by definition for this study, all TBI-cases demonstrated with an intracranial hematoma, categorized as epidural, subdural, subarachnoid, or intracerebral. Three out of nine TBI and fracture patients (33%) developed a hypertrophic callus (TBI + Fx + Call) within 14 to 24 days after admission to the hospital (diagnosed by X-ray and CT-scan), which was characterized by an excessive accumulation of cartilaginous and/or fibrous tissue at a fracture site. The remaining six patients with TBI and fracture (TBI + Fx) did not exhibit accelerated callus formation, instead demonstrating normal fracture healing.

TBI-associated hypertrophic callus-formation is most commonly observed in long-bone fractures. In addition to increased bone-mass-formation, it is usually accompanied with accelerated fracture union and occasionally with heterotopic ossification[25]. In this study, one TBI-fracture-patient developed a hypertrophic callus after sustaining a facial fracture (mandible) and was therefore assigned to the TBI + Fx + Call group.

DLK1-DIO3 cluster miRNA levels are increased in serum of hypertrophic callus patients 24 h after injury

Three representative patient samples of each group (see Table 1 and methods section) were chosen for small-RNA-seq and miRNA expression analysis. We analyzed serum miRNA levels at three different time points after admission to the hospital (24 h, 72 h and 7d) in all four patient groups (Supplementary Tables S1–S3; supplementary Figs. S1 and S2). Of all pairwise group comparisons (see Supplementary Table S4), for this study we focused on miRNAs that were differentially regulated in TBI + Fx patients who developed a hypertrophic callus, aiming to identify a distinct molecular signature associated with aberrant fracture healing. The resulting top ten candidate miRNAs were then chosen for downstream analyses (Fig. 3A). The time course progression of these miRNAs was validated by qPCR and demonstrated increased serum levels in patients with hypertrophic callus formation as early as 24 h post admission to the hospital. Two miRNAs, hsa-miR-1246 and hsa-miR-1291, were downregulated in accordance with RNA-seq data (Fig. 3B). hsa-miR-10a-5p could not be detected by the miRNA-assay in any sample and was excluded from all consecutive analyses.

Further analysis revealed that seven out of nine remaining candidate miRNAs originate from the same genomic locus, a parentally imprinted cluster of protein-coding genes, lncRNAs, snoRNAs and miRNAs on human chromosome 14q32 (C14q32), also known as *DLK1-DIO3* cluster (Fig. 3C). While this cluster has been reported in various biological contexts[22], it has not yet been associated with altered bone fracture healing in combination with traumatic brain injury.

Candidate DLK1-DIO3 miRNA levels are increased in sera of callus-patients compared to non-callus-patients and to healthy controls

To verify and identify the most strongly deregulated miRNAs associated with hypertrophic callus-formation, we expanded our dataset and analyzed the expression of candidate miRNAs by qPCR in serum samples retrieved 24 h-post-injury for individual patients of all four groups included in our study. The 24 h timepoint was chosen, since differences in expression were highest at that timepoint in the RNA-seq analysis, and the expression decreased at later timepoints except for hsa-miR-543, which showed highest expression 72 h post injury. Furthermore, we included healthy controls to identify the base-level-expression of the candidate miRNAs.

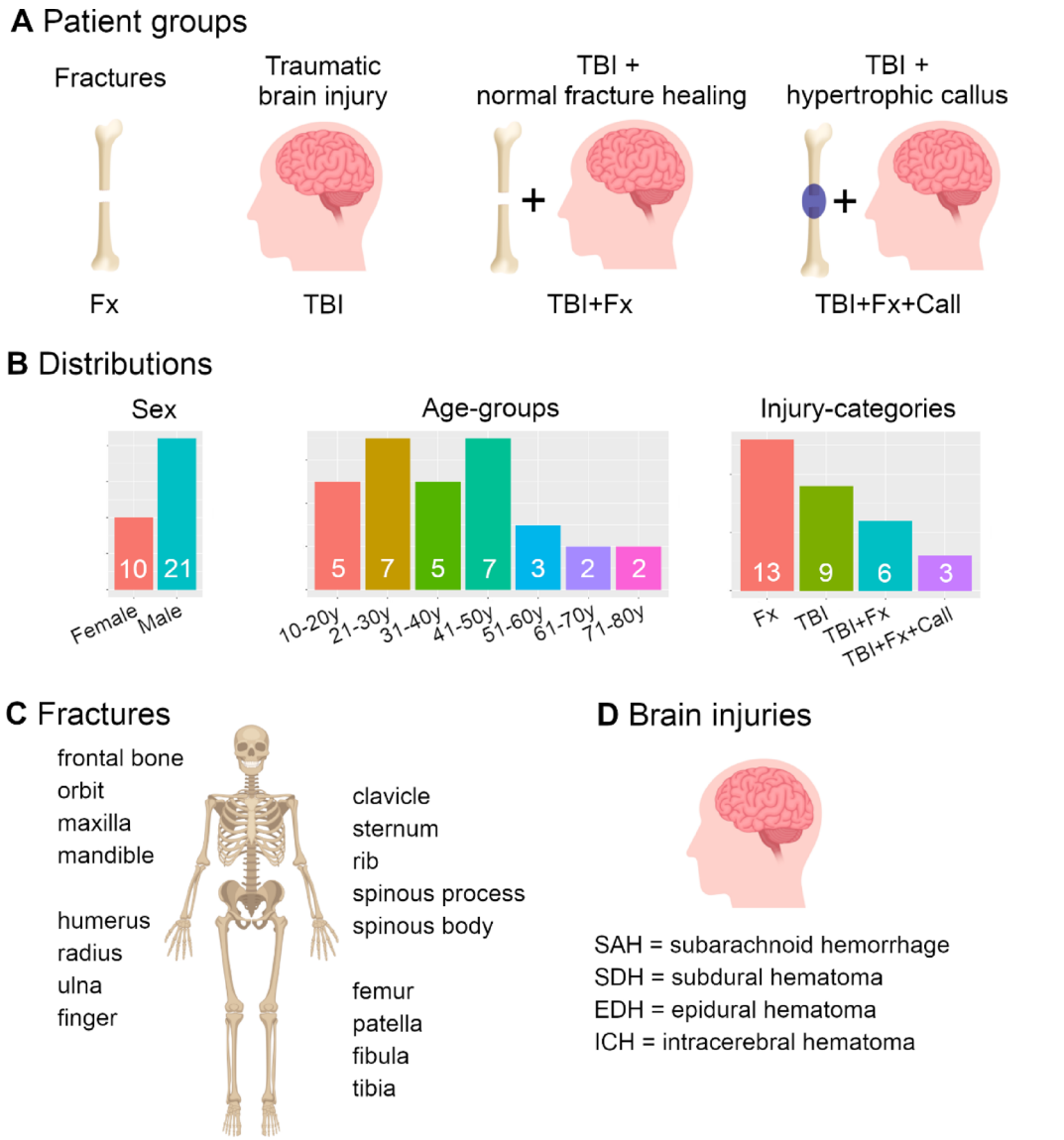

Fig. 1. Patient groups and injuries. (**A**) Patients were assigned to four groups: Fractures (Fx), traumatic brain injury (TBI), TBI with fractures and normal fracture healing (TBI + Fx) and TBI with fractures and formation of a hypertrophic callus (TBI + Fx + Call). (**B**) Total counts for gender distribution (left), age groups (center) and injury categories (right). (**C**) Fracture locations and (**D**) definitions of head injury abbreviations.

Except for hsa-miR-654-5p, the expression of all DLK1-DIO3 cluster miRNAs was significantly increased in TBI + Fx + Call patients compared to TBI + Fx patients and to healthy controls. Expression in Fx and TBI groups showed no statistically significant change compared to any other group or to healthy controls. (Fig. 4A; supplementary Table S5). Interestingly, the expression of DLK1-DIO3 miRNAs in TBI + Fx patients was as low as in healthy controls, either being not detectable or almost not present. The two miRNAs that are not encoded on the DLK1-DIO3 cluster, hsa-miR-1246 and hsa-miR-1291, showed different expression trends compared to the miRNA-seq results. Instead of being decreased in TBI + Fx + Call patients, their expression showed either no significant difference compared to TBI + Fx patients or a slight upregulation of hsa-miR-1246 compared to healthy controls.

To evaluate the feasibility of our candidate miRNAs as potential markers for hypertrophic callus-formation, we performed principal component analysis (PCA), which revealed a clear separation of TBI + Fx + Call from TBI + Fx and healthy controls (Fig. 4B). Orthogonal partial least squares discriminant analysis (oPLS-DA) further revealed that candidate miRNAs from the DLK1-DIO3 cluster but not hsa-miR-1246 and hsa-miR-1291 primarily contributed to the variance observed between TBI + Fx + Call and TBI + Fx patients (Fig. 4C; supplementary Fig. S3).

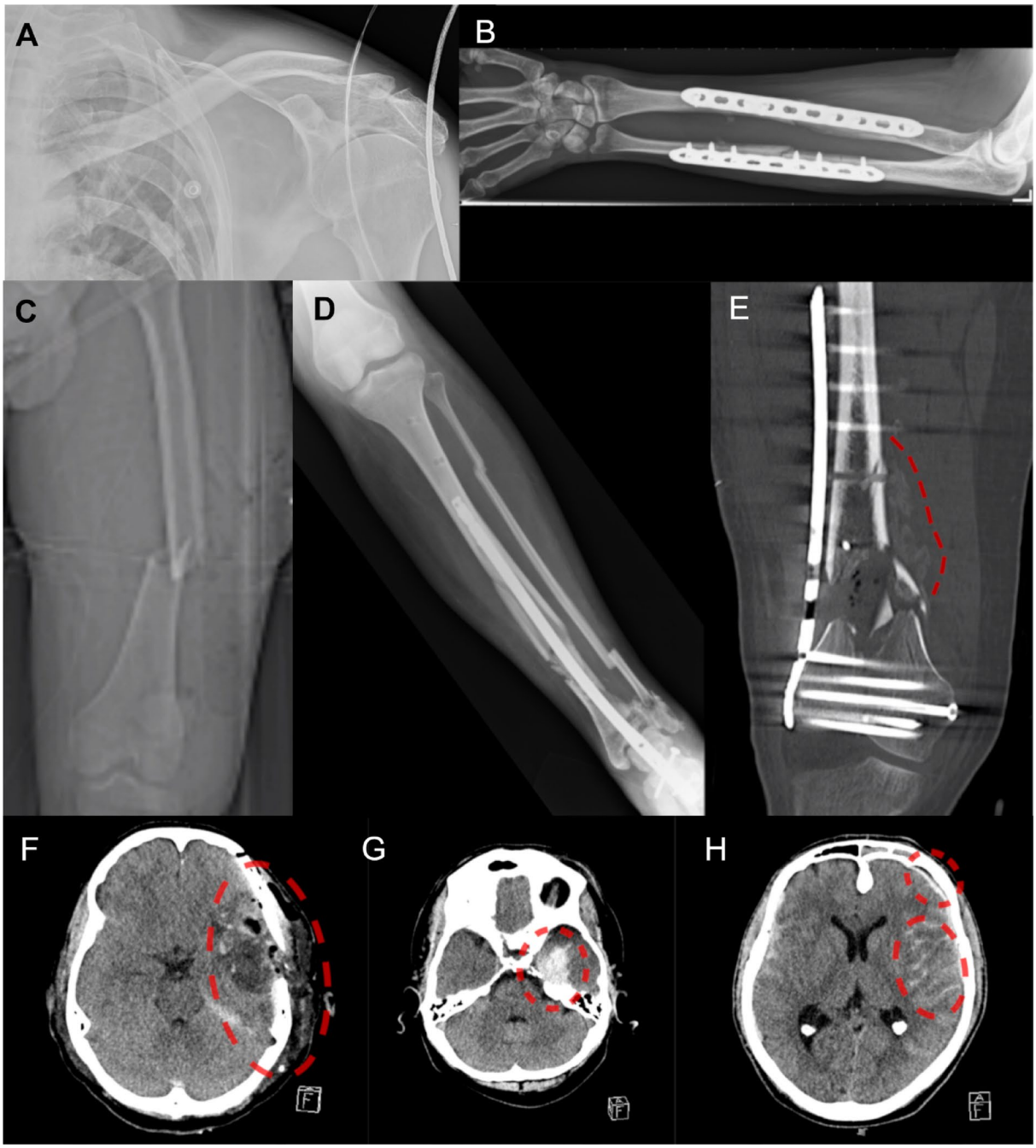

Fig. 2. X-ray and CT images of injuries. Representative examples of injuries from patients included in the study. (**A**) Anterior–posterior (AP) X-ray of a lateral clavicle fracture (patient 019). (**B**) AP X-ray of a forearm fracture (radius and ulna; patient 016). (**C**) Frontal CT scan of a femoral shaft fracture (patient 006). (**D**) AP X-ray of an open tibial shaft fracture including the pilon (patient 029). (**E**) AP X-ray of an open distal femur fracture with hypertrophic callus marked with a red dashed line (patient 032). (**F**) TBI, SDH, ICH (patient 001). (**G**) TBI, SDH (patient 028). (**H**) TBI, SDH, SAH (patient 019). Head injuries in F, G and H are marked with red dashed circles.

Pituitary gland extract induces the expression of candidate miRNAs in hBMSCs in vitro

To investigate the biological role of our candidate miRNAs, we performed GO-term analysis and found a strong association with brain development and synaptic activity for the mRNA-targets of hsa-miR-376a-3p, hsa-miR-487b-3p, hsa-miR-543, hsa-miR-654, hsa-miR-1246 and hsa-miR-1291. Pathways related to bone biology, such as Wnt-signaling, cartilage and connective tissue development, SMAD signaling, growth factor receptor binding and GTPase activity was evident for mRNA targets of hsa-miR-543, hsa-miR-1246, hsa-miR-376a-3p and hsa-miR-411-5p. Except for hsa-miR-411-5p, the three latter miRNAs are categorized by overlapping functions in

Patient-ID	Group	small-RNA-seq	Sex	Age	Fractures and TBI
P004	Fx	Seq	F	43	Humeral shaft , Forearm (ulna and radius), Pelvic ring, Femoral shaft and trochanteric, Distal femur, Calcaneus
P006	Fx	Seq	M	27	Femoral shaft , Tibial shaft
P011	Fx		M	48	Distal femur, Patella
P012	Fx		M	16	Humeral shaft
P013	Fx		F	17	Femoral shaft , Patella
P014	Fx	Seq	F	38	Femoral shaft
P017	Fx		F	72	Distal femoral shaft
P018	Fx		M	37	Humeral shaft
P021	Fx		M	21	Forearm (ulna, radius)
P022	Fx		M	35	Humeral shaft
P025	Fx		M	18	Femoral shaft (both sides)
P033	Fx		F	44	Humeral shaft, Monteggia like (radial head, ulna shaft), Pelvic ring , Femoral shaft, Tibial shaft (both sides)
P034	Fx		M	27	Monteggia like (ulna Schaft and olecranon), Femoral shaft
P001	TBI	Seq	M	19	severe TBI, SDH, Intracebreral hematoma
P003	TBI		M	48	severe TBI, SAH, SDH
P007	TBI		M	36	severe TBI, SDH
P008	TBI	Seq	F	38	severe TBI, EDH, SAH
P009	TBI		M	57	severe TBI, Intracerebreral hematoma
P010	TBI		M	61	severe TBI, SAH, Intracerebreral hematoma
P027	TBI		M	46	severe TBI, SAH
P028	TBI	Seq	M	29	severe TBI, SDH
P030	TBI		M	24	severe TBI , SDH, SAH
P015	TBI + Fx		M	16	severe TBI, SDH, Clavicle shaft, Distal radius, Spinal
P016	TBI + Fx	Seq	F	41	severe TBI, SAH, Clavicle, Scapula, Proximal humerus, Forearm (ulna, radius), Proximal tibia
P020	TBI + Fx		F	64	severe TBI, SAH, Distal ulna
P026	TBI + Fx		M	80	severe TBI, Intracerebral hematoma, Subtrochanteric,, Femoral shaft
P029	TBI + Fx	Seq	F	29	severe TBI, SDH, Diffuse atonal injury, Tibial shafts (and fibula; both sides)
P031	TBI + Fx	Seq	F	58	severe TBI, SAH, Clavicle, Distal radius, Proximal tibia
P005	TBI + Fx + Call	Seq	M	41	severe TBI, EDH, SAH, Mandible
P019	TBI + Fx + Call	Seq	M	56	severe TBI, SDH, SAH, Proximal femoral, Lateral clavicle
P032	TBI + Fx + Call	Seq	M	27	severe TBI, SAH, Distal femoral (both sides), Olecranon, Patellar

Table 1. Patient demographics.

brain- and bone biology alike. The complete list of candidate miRNA-mRNA-targets and GO-term analysis results are documented in supplementary Table S6 and supplementary Fig. S4.

Based on the observation that our candidate miRNAs showed overlapping functions in brain- and bone-biology according to GO-term analysis, we investigated the overall expression of these miRNAs in human tissues using publically available miRNA-Tissue-Atlas data[26]. We noticed that all DLK1-DIO3 miRNAs are highly expressed in the human brain (Fig. 5, Supplementary Table S7). The non-cluster miRNA hsa-miR-1246 is not expressed in the brain and hsa-miR-1291 is not constitutively expressed significantly in any tissue at all. None of the candidate miRNAs shows significant expression in bone tissue.

Given that tissue expression data indicate high levels of most candidate miRNAs in the brain, we further examined various sub-regions of the human brain in detail. This analysis revealed a notable accumulation of DLK1-DIO3 candidate miRNAs in the pituitary gland (Fig. 6A; supplementary Table S8). To explore a potential relation further, we incubated hBMSCs in the presence or absence of bovine pituitary gland extract (PGE) for 72 h and analyzed the expression levels of candidate miRNAs in cell lysates by qPCR. With the exception of hsa-miR-654-5p and hsa-miR-1291, the expression of all candidate miRNAs was significantly increased when hBMSCs were cultured in the presence of PGE (Fig. 6B; supplementary Table S9).

Candidate miRNA hsa-miR-543 represses RANKL expression

Based on the combined results from miRNA–target prediction, GO-term enrichment (Supplementary Fig. S4), and VIP score analysis derived from oPLS-DA (Fig. 4C), hsa-miR-543 emerged as one of the principal candidate miRNAs within the potential biomarker set distinguishing serum samples from TBI + Fx + Call and TBI + Fx patients (Supplementary Fig. S3). Among its predicted mRNA targets is RANKL (TNFSF11; Fig. 7A), a key regulator of osteoclast differentiation and bone remodeling. To further investigate its functional relevance, hBMSCs from three individual donors were transfected in vitro with a hsa-miR-543 mimic. In line with the in-

A small-RNA-seq

miRNA	logFC	logCPM	F	pValue	FDR
hsa-miR-127-3p	-1.4	5.3	18	3.5e-04	0.0160
hsa-miR-376a-3p	-1.6	6.8	17	4.5e-04	0.0160
hsa-miR-411-5p	-1.6	5.2	26	4.9e-05	0.0049
hsa-miR-431-5p	-1.4	4.4	13	1.5e-03	0.0340
hsa-miR-487b-3p	-1.6	7.0	16	5.9e-04	0.0160
hsa-miR-543	-1.6	6.0	17	4.7e-04	0.0160
hsa-miR-654-5p	-2.2	5.6	38	4.8e-06	0.0011
hsa-miR-1246	1.3	11.0	16	7.3e-04	0.0180
hsa-miR-1291	2.3	4.1	16	5.9e-04	0.0160
hsa-miR-10a-5p	1.5	5.1	23	1.1e-04	0.0066

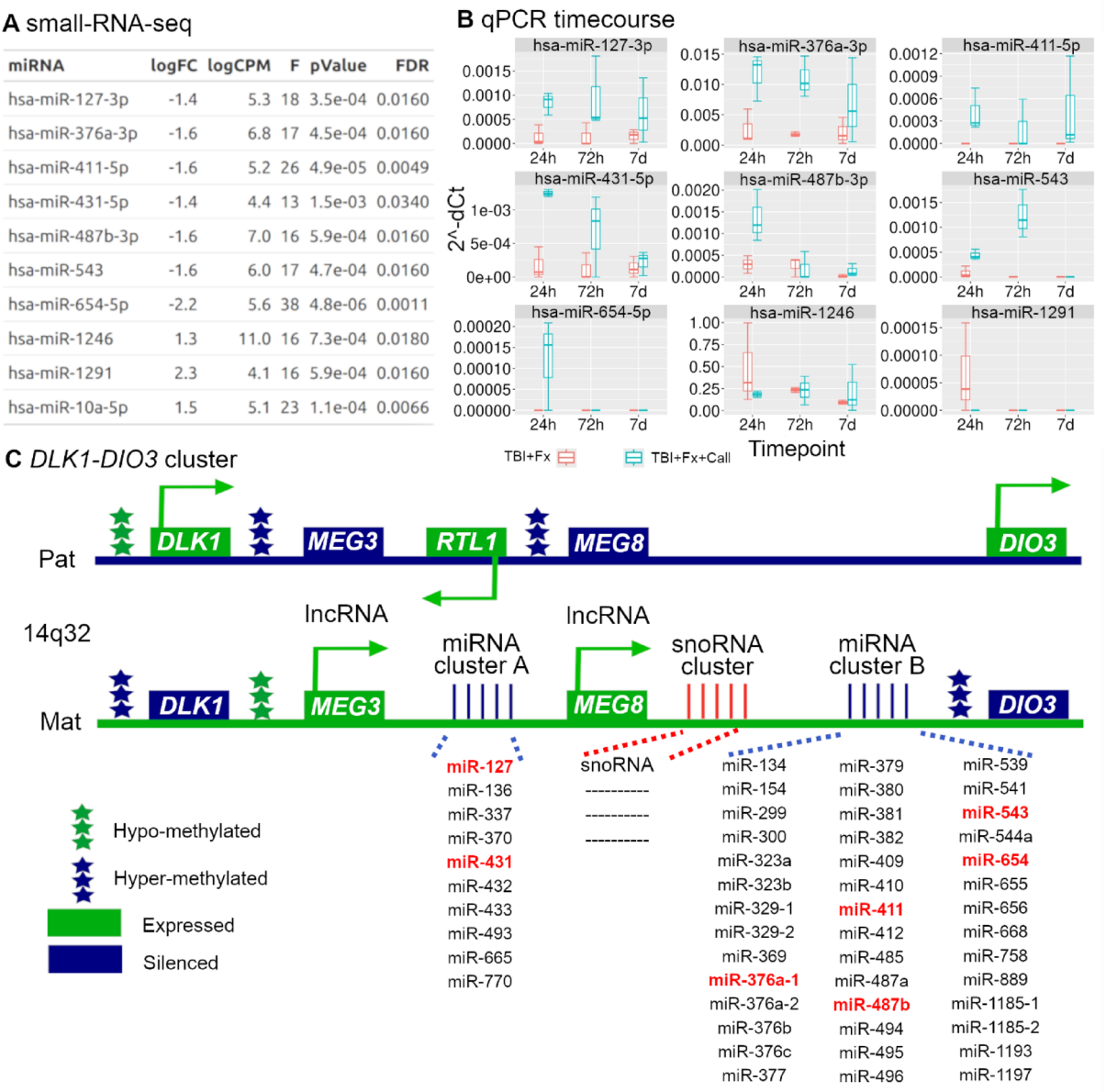

Fig. 3. Small-RNA-seq analysis and DLK1-DIO3 cluster miRNAs. (**A**) Top 10 miRNA candidates differentially expressed between TBI + Fx and TBI + Fx + Call samples 24 h after injury. Positive logFC indicates higher expression in TBI + Fx. Hsa-miR-10a-5p could not be confirmed by RT-qPCR and was excluded from all consecutive analyses. (**B**) qPCR shows the time course progression of candidate miRNAs in patient sera 24 h, 72 h and 7d after injury. Except for hsa-miR-1246 and hsa-miR-1291 all miRNAs are highly expressed in TBI + Fx + Call patients 24 h after injury. Hsa-miR-543 shows highest expression 72 h after injury. Expression of all miRNAs in TBI + Fx + Call decreases with progressing time, whereas expression in the TBI + Fx group remains low at all timepoints, except for hsa-miR-1246 and hsa-miR-1291. Boxplots indicate datapoints of the three patients in each group that were subject to small-RNA-seq analysis. (**C**) The DLK1-DIO3 cluster on human chromosome 14q32. Maternal and paternal genomic imprinting is indicated by color code (green = hypo-methylated and expressed; blue = hyper-methylated and silenced). Candidate miRNAs of this study are encoded on the miRNA clusters A and B and are indicated in red.

silico predictions, RANKL protein levels showed a trend toward downregulation compared to negative controls (Fig. 7B; Supplementary Fig. S5).

In-silico analysis further revealed that several of the predicted miRNAs target mRNAs/proteins (Supplementary Table S6) that are potentially not only involved in the RANKL pathway (e.g., RANKL, RANK, TRAF6, MAPK1), but also the BMP-RUNX2-axis (e.g., BMP-2, BMPR, SMAD2/4, RUNX2), PI3K-AKT signaling axis (e.g., PI3K, AKT1/2/3), and the Wnt/β-catenin pathway (e.g., SOST, WNT1, LRP6, CTNNB1). These findings suggest that several of the identified candidate miRNAs may impact on bone formation and

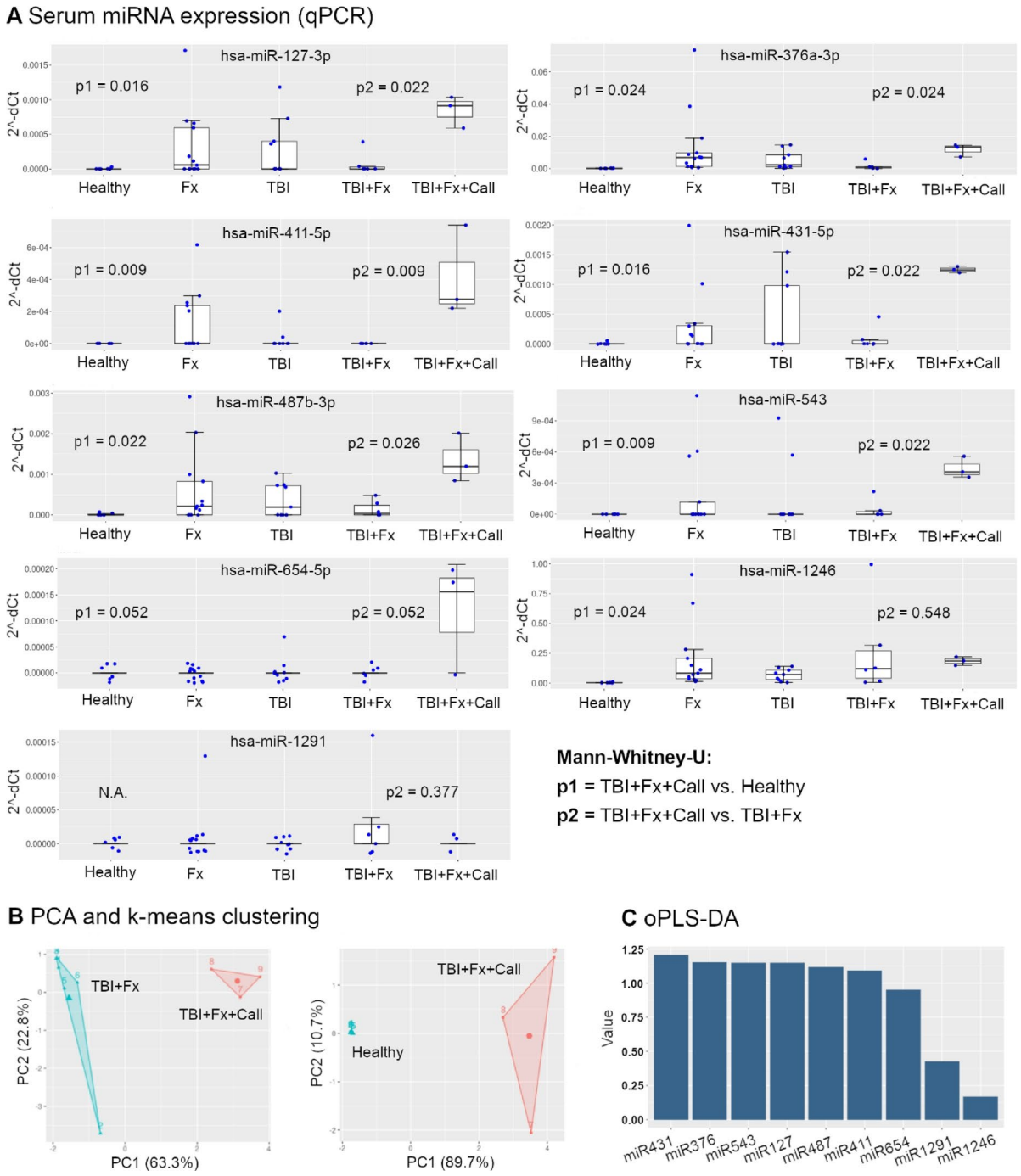

Fig. 4. Candidate miRNA expression in sera of patients and healthy controls. (**A**) Absolute expression of miRNAs in patient and healthy control sera 24 h after injury. Expression of all DLK1-DIO3 miRNAs, except hsa-miR-654-5p, was significantly increased in TBI + Fx + Call patients compared to TBI + Fx patients and healthy controls. Micro-RNAs hsa-miR-1246 and hsa-miR-1291 did not show the same trend as in the RNA-seq analysis. Data are given as 2^{-dCt} values in box-plots depicting individual data points. Non-parametrical Mann–Whitney-U test was used for pairwise comparisons (Healthy: n = 6. Fx: n = 13. TBI: n = 9. TBI + Fx: n = 6. TBI + Fx + Call: n = 3). (**B**) PCA and k-means clustering shows a clear separation of callus-patients compared to non-callus-patients and healthy controls. (**C**) Variable importance in projection (VIP) plot with data generated from oPLS-DA analysis shows to which extend candidate miRNAs from the DLK1-DIO3 cluster, but not hsa-miR-1246 and hsa-miR-1291, contribute to the variance between TBI + Fx + Call and TBI + Fx patients.

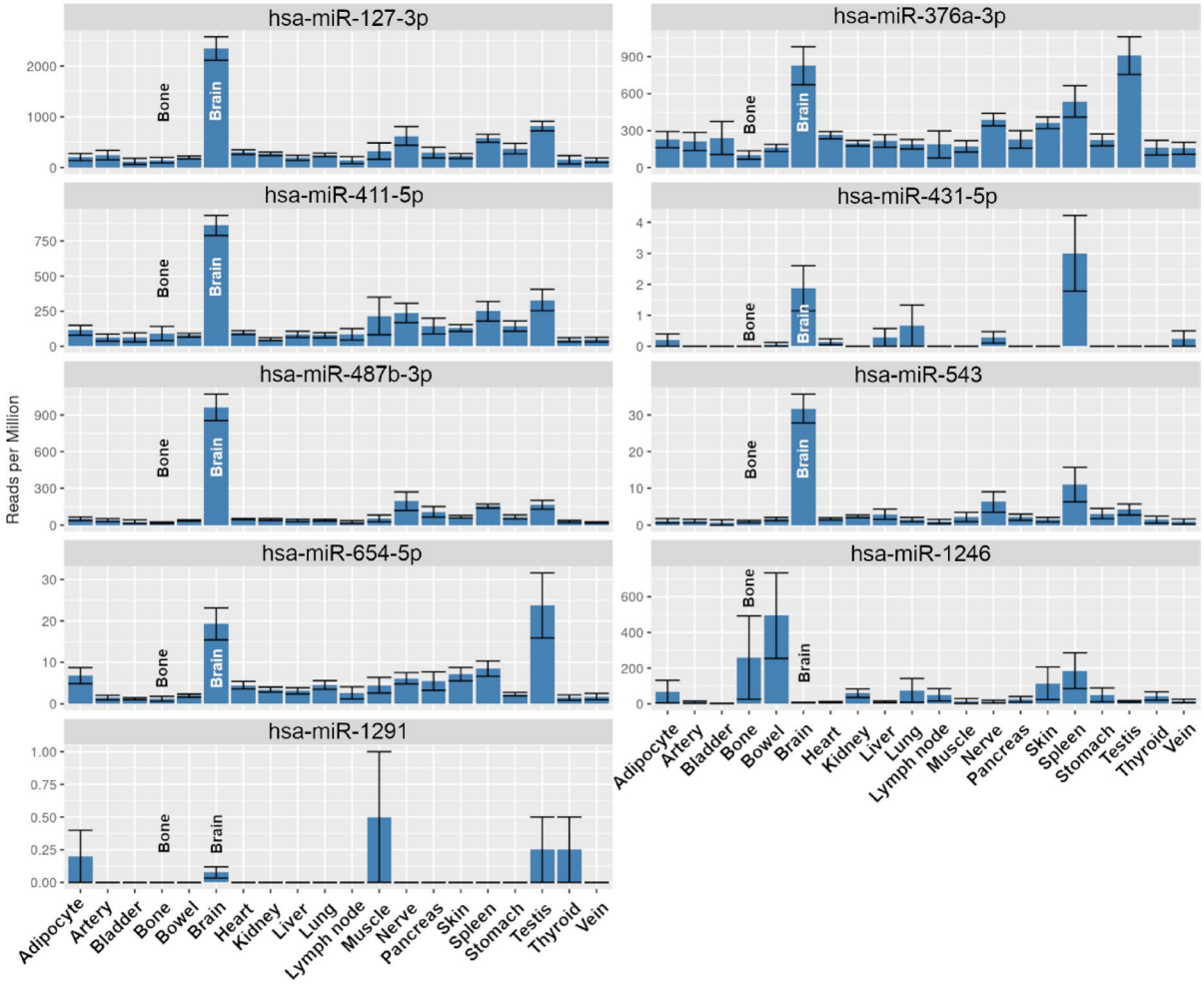

Fig. 5. Candidate miRNAs are highly expressed in the human brain. Except for hsa-miR-1246 and hsa-miR-1291, all miRNAs investigated in this study show high expression in the human brain. None of the candidate miRNAs is significantly expressed in bone. Data obtained from miRNA-Tissue-Atlas[26]. Bars = absolute counts, normalized as reads per million. Errorbars = SD. Explorative data without statistical analysis.

remodeling, although this requires further experimental validation. Further, not all candidate miRNAs are expected to be active simultaneously or at the same anatomical site, however, their broad involvement supports a potential role in TBI-related hypertrophic callus formation and warrant further investigation.

Discussion

The identification of causal factors underlying TBI-associated hypertrophic callus formation remains an ongoing area of research. In this study, we identified a set of systemic miRNAs which could serve as promising biomarkers for predicting hypertrophic callus formation at an early stage following TBI-related injuries.

The involvement of DLK1-DIO3 miRNAs in fracture healing and osteogenic pathways has been recently shown. In 2023, the study from Hadjiargyrou et al.[28] identified miR-127-3p and miR-654-5p to be highly expressed in fracture callus-tissue during physiological healing and a recent study from the Stoddard group[29], found differentially regulated miRNAs located within the DLK1-DIO3 cluster in serum of fracture-patients and conditioned culture medium of osteogenically induced hBMSCs. The latter study found hsa-miR-1246 to be elevated at all time-points of fracture healing, along with a number of DLK1-DIO3 miRNAs, which were similarly found to be regulated in the patients from our study. However, neither study aimed to investigate the role of these miRNAs in the context of TBI-related fracture healing or demonstrated their origin from the DLK1-DIO3 cluster. Therefore, the findings of our study not only build upon these previously published results, but also provide new insights into potential biological roles of these miRNAs.

A number of studies already investigated the miRNA-composition of mild, moderate and severe TBI in serum/plasma, cerebrospinal fluid and in saliva. In none of these studies, C14q32 cluster miRNAs or hsa-miR-1246 and hsa-miR-1291 appeared to be differentially regulated. Why these miRNAs have not been identified in TBI so far and the lack of understanding from which tissue/cells they originate in patients with hypertrophic callus formation after having sustained a traumatic brain injury may be the consequence of differences in

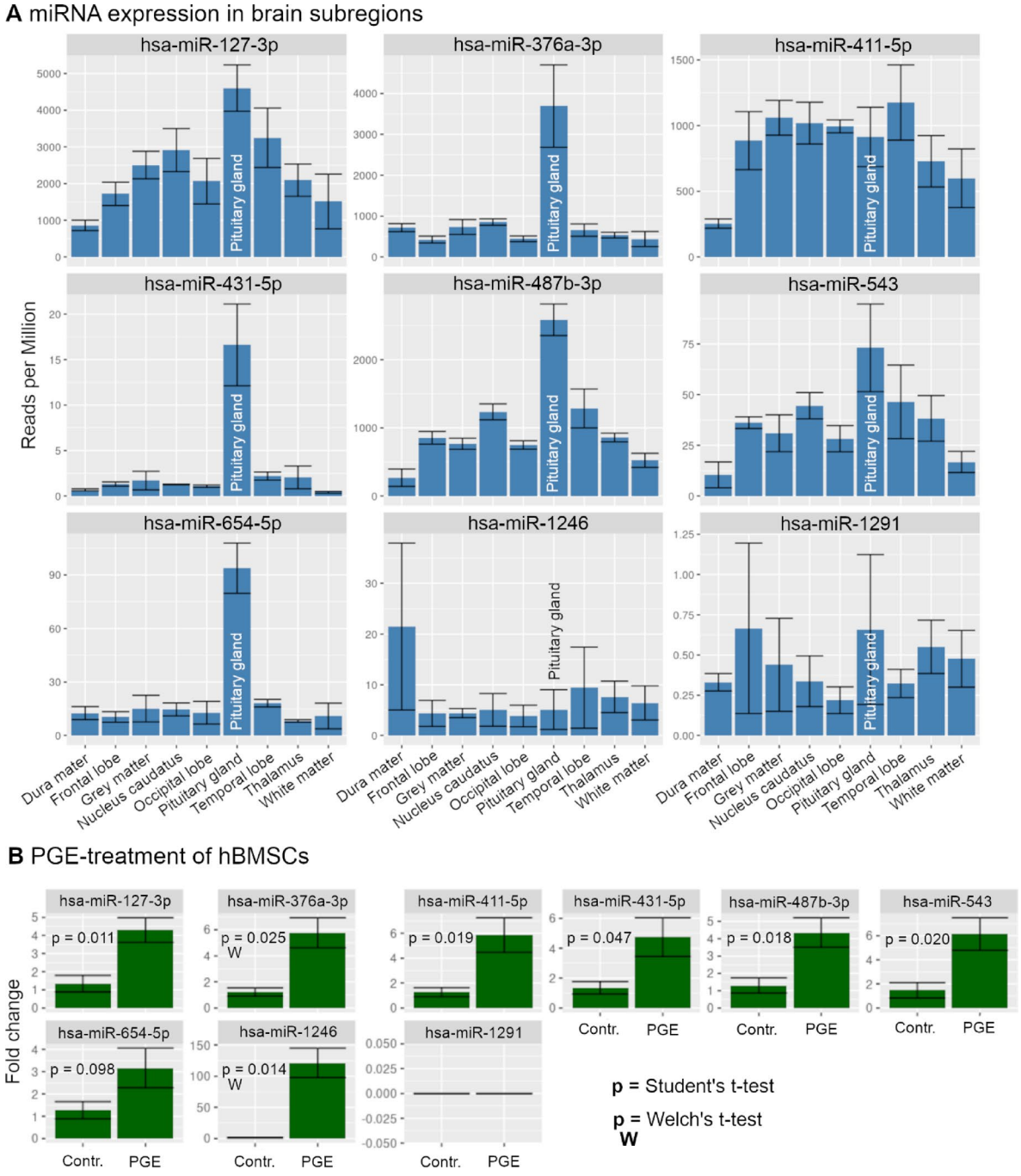

Fig. 6. Candidate miRNAs are functionally connected to the pituitary gland. (**A**) Candidate miRNAs are highly expressed in the pituitary gland. Data obtained from miRNA-Tissue-Atlas[26]. Bars = absolute counts, normalized as reads per million. Errorbars = SD. Explorative data without statistical analysis. (**B**) hBMSCs were cultured in presence (PGE) or absence (Contr.) of 70 µg/ml bovine pituitary gland extract for 72 h. Expression of miRNAs was assessed by qPCR (n = 4, bars = arithmetic mean, errorbars = SEM. Either Student's t-test or Welch's t-test were applied for pairwise comparison).

study designs and methodologies employed. Some studies used assays with pre-defined panels of miRNAs that did not include any of the miRNAs of the present study[19,30]. A majority of studies solely focused on murine models[31–34] or investigated the miRNA expression patterns of TBI in humans in specific neurologic contexts that are not comparable to our study[18,35]. Another critical aspect is the timing of blood sampling. We observed that serum miRNA expression levels were highest at the early 24 h timepoint and declined progressively thereafter, suggesting that delayed sampling may fail to capture relevant miRNA signatures.

All fractures heal with a thickening callus at the fracture site, which is subsequently resorbed in a controlled manner during the remodeling phase of fracture healing[36]. A TBI-associated hypertrophic callus, on the other

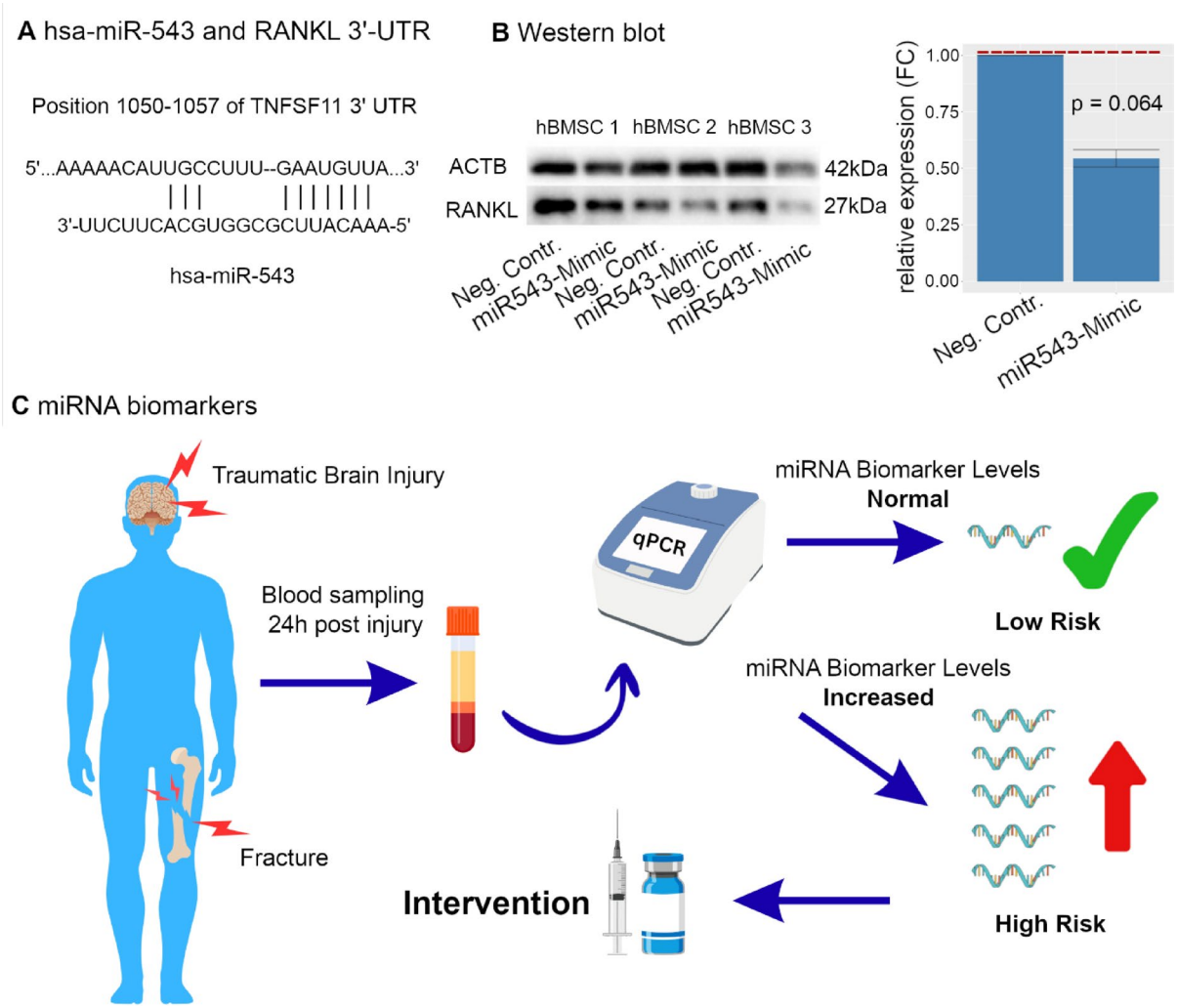

Fig. 7. Candidate miRNAs in osteogenic pathways. (**A**) The 3'-UTR of RANKL (TNFSF11) together with hsa-miR-543 bound at position 1050–1057 (sequence information obtained from TargetScanHuman.8.0[27]). (**B**) Western blot of hBMSCs from three individual donors. Cells were either transfected with 25 nM hsa-miR-543-mimic or with a negative control. The effect varies in degree between the three hBMSCs, and the foldchange computed from densitometric analysis is close to statistical significance ($p = 0.064$, Mann–Whitney-U test). Original, uncropped, Western blot and densitometric data are provided in supplementary Fig. S5. (**C**) Schematic overview illustrating potential of identified miRNA biomarker candidates for early risk stratification after trauma.

hand, is not only increased but occasionally remains and requires surgical debridement. The miRNAs identified in our study, their mRNA-targets and their affected pathways potentially offer new insights underlying this phenomenon.

In this study, we demonstrate, to the best of our knowledge for the first time, that treatment of BMSCs with a hsa-miR-543 mimic leads to reduced expression of RANKL. Interestingly, a previous study demonstrated that treatment with either the bisphosphonate alendronate or inhibition of RANKL using the humanized monoclonal antibody denosumab resulted in an increased final callus size in a mouse femoral fracture model[37]. In silico analyses further indicate that several of the identified candidate miRNAs may downregulate proteins involved in bone formation and remodeling; however, these predictions remain to be experimentally validated and thus lie beyond the scope of the present work. Moreover, whether the systemic increase of these miRNAs observed as early as 24–72 h post-injury contributes to hypertrophic callus formation in polytraumatized patients remains unclear and warrants further investigation.

In silico analysis showed marked accumulation of DLK1-DIO3 miRNAs in the human pituitary gland, potentially suggesting an endocrine contribution to the increase in callus formation in TBI patients. Consistently, pituitary gland extract (PGE) induced upregulation of several candidate miRNAs in hBMSCs. As these effects cannot be ascribed to defined PGE components, the findings remain descriptive, and mechanistic insights will require systematic analysis of individual pituitary factors and analysis of additional patient sera in future

studies. The strong pituitary expression is however noteworthy, as prolactin has been proposed as a link between traumatic brain injury and hypertrophic callus formation[38].

The major limitation of our study is undoubtedly the small sample size, with only three patients presenting hypertrophic callus formation. However, the observation that approximately one third of patients who had sustained a TBI and bone fracture(s) develop a hypertrophic callus is in good approximation with the numbers reported from a similar study where collagen degradation, delayed fracture union and increased osteogenesis were investigated in patient groups comparable to ours[25]. Despite the small sample size, we were able to demonstrate that differences in miRNA expression between hypertrophic callus and non-callus patients as well as healthy controls are statistically significant with only few exceptions. However, future studies involving larger cohorts are essential to substantiate and validate our findings. Such studies will be crucial to confirm the identified set of miRNAs as definitive markers associated with hypertrophic callus formation and to establish serum thresholds or cutoff values suitable for clinical diagnosis. Further, future studies should not only include larger cohorts but also encompass additional OMICs methodologies, an expanded range of clinical diagnostic analyses, and careful consideration of factors such as gender and age. Furthermore, a thorough evaluation of patients' medical histories will be critical to providing a more nuanced understanding of the observed phenomena and their potential clinical implications.

In conclusion, the identified DLK1-DIO3 cluster miRNAs show significantly increased serum levels in hypertrophic callus patients as early as 24–72 h post-injury. While these signatures may not be causally linked to the underlying biological mechanisms driving hypertrophic callus formation, their early regulation highlights their potential as serological biomarkers to predict excessive callus formation (Fig. 7C). Such biomarkers could provide valuable clinical tools to identify patients at risk before radiographic signs of hypertrophy become apparent, allowing personalized therapeutic interventions.

Methods

Ethics statement

This study included blood samples of human subjects and was approved by the Ethics Commission for the State of Salzburg (approval number 415-E/2293/4-2018). Due to the critical condition of traumatic brain injury patients at the time of admission to the hospital (unconscious due to head injury or through medically induced coma), blood sampling at the University Hospital Salzburg, Austria was performed with written informed consent of a legal guardian. All experiments that included human subjects were performed in accordance with the *World Medical Association Declaration of Helsinki—Ethical Principles for Medical Research Involving Human Subjects*[39]. No animal experiments were conducted in this study. No large language models (LLM) were used in the generation or analyses of data or for writing the manuscript.

Patient inclusion and exclusion criteria

Inclusion-criteria

Patients with one or several long-bone fractures. Patients with isolated traumatic brain injury with confirmed intracranial bleeding with or without fracture of the skull including craniomaxillary fractures. Patients with long-bone fractures accompanied with traumatic brain injury with confirmed intracranial bleeding with or without fracture of the skull.

Exclusion-criteria

Patients with fractures of only small bones. Patients with isolated traumatic brain injury without confirmed intracranial bleeding. Patients with chronic illnesses of the central nervous system. Patients with muscular-skeletal illnesses. Patients with metabolic illnesses. Patients with ongoing immune-suppressive therapy or ongoing treatment with bisphosphonates. Children under the age of 16 years. Pregnancy.

Blood sampling

Blood samples were taken at the University Hospital Salzburg, Austria, at the following time-points: within 6 h after injury; at 24 h, 72 h, 7 days and 14 days after injury. Peripheral blood was collected in a BD Vacutainer®, clotted for 30 min and then centrifuged at 2.500*g* for 10 min. At least three serum aliquots (0.5 ml each) were stored at -20 °C short term, transferred to the laboratory and stored at -80 °C long term. After thorough instruction of the medical team, blood sampling started with May 2018 and continued for a period of three years until April 2021. Healthy control serum samples were kindly provided by the Department of Dermatology and Allergology of the University Hospital Salzburg.

RNA extraction from serum and cell-lysates

Total RNA was extracted from human blood samples using miRNeasy Serum/Plasma Advanced Kit (qiagen, #217204) according to manufacturer's protocol. Total RNA from cell lysates was extracted using TRI-Reagent (MRC, #TR118) followed by chloroform extraction and isopropanol precipitation according to standard protocols.

Small-RNA-seq analysis

Micro-RNA-seq analysis was performed by a contractor (TAmiRNA GmbH, Leberstrasse 20, 1110 Vienna, Austria) according to their customized protocol. RNA preparation and library construction was performed using Serum/Plasma Advanced Kit (Qiagen, #217204) and Biofluids Plasma/Serum miRNA Library kit (RealSeq, #600-00048) according to manufacturer's protocol. Sequencing was performed on an Illumina platform (NextSeq 550, 75 bp, SR). Analysis parameters were defined as follows: Sequencing adapter: RealSeq (cutadapt -a Realseq3P = TGGAATTCTC -u1). Minimum read length: 17nt. Reads quality cutoff: 30 (phred quality score). Significance

level: 0.05. Overall quality of the next-generation sequencing data was evaluated automatically and manually with fastQC v0.11.9 and multiQC v1.10. Reads from all passing samples were adapter trimmed and filtered using cutadapt v3.3. Reads were then filtered for a minimum length of 17 nucleotides. Mapping was performed with bowtie v1.3.0 and miRDeep2 v2.0.1.2, whereas reads were mapped first against the genomic reference GRCh38.p12 provided by Ensembl allowing for two mismatches and subsequently miRBase v22.1, filtered for miRNAs of hsa only, allowing for one mismatch. For a general RNA composition overview, non-miRNA mapped reads were mapped against RNAcentral and then assigned to various RNA species of interest. Statistical analysis of preprocessed NGS data was done with R v4.0 and the packages pheatmap v1.0.12, pcaMethods v1.82 and genefilter v1.72. Differential expression analysis with edgeR v3.32 used the quasi-likelihood negative binomial generalized log-linear model functions provided by the package. The independent filtering method of DESeq2 was adapted for use with edgeR to remove low abundant miRNAs and thus optimize the false discovery rate (FDR) correction.

The selection of the three representative patient samples for RNA-seq was primarily based on age and clinical presentation, which allowed us to achieve the closest possible matching across groups. While sex was considered where feasible, a complete match could not be achieved due to the composition of the available patient pool (e.g., only male patients in the TBI + FX + Call group, predominantly female patients in the TBI + FX group). The selected samples therefore represent the most clinically comparable cases available. Patient-IDs for small-RNA-seq: Fx (P004, P006, P014), TBI (P001, P008, P028), TBI + Fx (P016, P029, P031), TBI + Fx + Call (P005, P019, P032).

Cell culture

Human bone-marrow-derived mesenchymal stem cells (hBMSCs) were kindly provided by the Ludwig Boltzmann Institute for Traumatology (Vienna, Austria), and by the GMP core facility at Paracelsus Medical University, (Salzburg, Austria). Samples were stored in liquid nitrogen (hBMSC-1: female, age 29, passage 1; hBMSC-2: female, age 27 passage 0; hBMSC-3: male, age 35, passage 0; hBMSC-4: female, age 20, passage 2). All in vitro experiments were performed at passage 5. Proliferation medium for primary cultures contained DMEM high glucose (gibco, #11960-044), 10% FBS (sigma, #F7524-500ML), 1 × Glutamax (gibco, #350500-038), 1 × Penicillin/Streptomycin (sigma, #P4333-100ML) and 1 ng/ml bFGF (peprotech, #AF-100-18B-50UG). Cells were cultured at 37 °C and 5% CO_2 in a humidified atmosphere. Medium was changed every second day and cells were passaged at 90% confluence with 0.125% trypsin/EDTA (sigma, #T4049-500ML).

Pituitary gland extract treatment

Treatment of hBMSCs with bovine pituitary gland extract (PGE, Gibco, #13028014) was conducted as follows: 2×10^4 hBMSCs (hBMSC-1, hBMSC-4) were seeded in 12-well cell-culture plates in duplicates (total n = 4). Untreated control samples were cultured in α-modified MEM Eagle (PAN Biotech, #P04-21050) supplemented with 1 × Glutamax, 10% FBS (sigma, #F7524-500ML) and 1 × Penicillin/Streptomycin. PGE-treated samples were incubated in the same medium, supplemented with a final concentration of 70 µg/ml PGE. All samples were cultured for 72 h with one medium change in between. Cells were finally lysed in TRI-Reagent and RNA was extracted as described above.

Micro-RNA-mimic

Transfection of hBMSCs with a hsa-miR-543 mimic was conducted as follows: 2×10^4 cells of hBMSC-1, hBMSC-2 and hBMSC-3 were seeded in 12-well cell-culture plates in triplicates the day before the experiment and cultured in α-modified MEM Eagle (PAN Biotech, #P04-21050) supplemented with 1 × Glutamax and 1 × Penicillin/Streptomycin but without FBS. Hsa-miR-543 mirVana™ miRNA Mimic (Invitrogen, #4464066; Assay MC13037) and mirVana™ miRNA Mimic, Negative Control #1 (Invitrogen, #4464058) were used in a final concentration of 25 nM in a total volume of 1 ml medium. The transfection solution was prepared in a mixture of Opti-MEM (Fisher scientific, #10149832) and Lipofectamine RNAiMax (Fisher scientific, #13778100) according to the RNAiMax protocol. All cells were incubated for 24 h. Cells were finally lysed in 100 µl RIPA-buffer (Pierce™, #89900) supplemented with 1 × protease inhibitor (Sigma, #P8340) and 1 × phosphatase inhibitor (Sigma, #P0044) and stored at -80 °C.

Micro-RNA expression assay

RNA from patient serum or cell culture lysates was diluted to a final concentration of 5 ng/µl and a total amount of 10 ng (2 µl per reaction) was used for cDNA preparation using miRCURY LNA RT kit (qiagen, #339340). Relative expression of miRNAs was assessed by qPCR on a BIO-RAD CFX96 thermocycler using miRCURY LNA SYBR® Green PCR kit (qiagen, #339346) and LNA miRNA PCR Assays for selected miRNAs following manufacturer's protocol. miRNA Assays used in this study: hsa-miR-1246 (qiagen/GeneGlobe ID-YP00205630), hsa-miR-10a-5p (qiagen/GeneGlobe ID-YP00204778), hsa-miR-127-3p (qiagen/GeneGlobe ID-YP00204048), hsa-miR-1291 (qiagen/GeneGlobe ID-YP02107164), hsa-miR-376a-3p (qiagen/GeneGlobe ID-YP00204508), hsa-miR-487b-3p (qiagen/GeneGlobe ID-YP00204489), hsa-miR-411-5p (qiagen/GeneGlobe ID-YP00204532), hsa-miR-543 (qiagen/GeneGlobe ID-YP00204447), hsa-miR-654 (qiagen/GeneGlobe ID-YP00204439) and hsa-miR-431-5p (qiagen/GeneGlobe ID-YP00204737). U6-snRNA (qiagen/GeneGlobe ID-YP02119464) and 5s-rRNA (qiagen/GeneGlobe ID-YP00203906) were tested as references for data normalization. Throughout all experiments, 5s-rRNA expression was more reliable and stable compared to U6-snRNA and therefore used for data normalization. Results are given either as $2^{-\Delta Ct}$ values or as fold changes calculated with the $2^{-\Delta\Delta Ct}$ method[40].

Western Blot

Cell lysates were prepared using RIPA-buffer (Pierce™, #89900) supplemented with 1 × protease inhibitor (Sigma, #P8340) and 1 × phosphatase inhibitor (Sigma, #P0044). Protein concentration of cell-lysates was determined using BCA Protein Assay Kit (Pierce™, #23227). For initial SDS-PAGE and Western blot, 20 µg total protein per sample were electrophoretically separated on 10% gels (BIO-RAD TGX Stain Free FastCast Acrylamide Kit, #1610183), followed by transfer on PVDF-membranes (Sigma-Aldrich, #3010040001). Membranes were blocked for one hour in 5% milk powder in 1 × TBS-Tween. Primary antibodies were incubated over night at 4 °C. Membranes were washed with TBS-Tween and secondary antibodies were applied in 5% milk powder in TBS-Tween for one hour at room temperature. After washing away secondary antibodies, blots were developed in Clarity Max ECL Substrate (BIO-RAD, #1705062) and inspected on a gel-imaging system. In consecutive technical replicates, the protein amount was adjusted to achieve homogenous β-actin loading control bands. BIO-RAD Image Lab 5.2 software was used for densitometry and relative quantification of protein bands on blots. Antibodies used: Beta-actin (ACTB, Proteintech, #66009-1-Ig); RANKL (TNFSF11, Proteintech, #23408-1-AP); goat-α-mouse-HRP (BIO-RAD, #170-5047); goat-α-rabbit-HRP (BIO-RAD, #170-5046). Original, uncropped, Western blots are provided in supplementary Fig. S5.

Statistical- and bioinformatics analysis

Statistical parameters (sample-size, arithmetic mean, standard deviation or standard error, p-values etc.) are presented in the figures and figure legends. Statistical tests for pairwise comparison of samples were chosen based on the following considerations: A Shapiro–Wilk-test was performed to test for normality. If normal distribution was not the case, non-parametric Mann–Whitney-U-test was performed. In case of normality, homogeneity of variances was determined with Levene's test. Student's-t-test was chosen for data with homogenous variances; Welch's-t-test was chosen for inhomogenous variances. Pairwise comparisons are always *independent* and *two-sided*. Statistical analysis was only performed with biological replicates. R-statistical software (v4.4.2) and RStudio (v2024.09.0) were used for bioinformatic analysis of miRNA-targets, GO-term-analysis and for the creation of plots.

Data availability

Sequencing datasets generated and/or analysed during the current study are available in the GEO repository (GSE294842). In addition, all raw data, including small-RNA-seq data and qPCR-Ct-values are available in the supplementary tables.

Received: 25 March 2025; Accepted: 3 November 2025
Published online: 04 December 2025

References

1. Perkins, R. & Skirving, A. P. Callus formation and the rate of healing of femoral fractures in patients with head injuries. *J. Bone Joint Surg. Br.* **69**(4), 521–524 (1987).
2. Yang, T. Y., Wang, T. C., Tsai, Y. H. & Huang, K. C. The effects of an injury to the brain on bone healing and callus formation in young adults with fractures of the femoral shaft. *J. Bone Joint Surg. Br.* **94**(2), 227–230 (2012).
3. Calandriello, B. Callus formation in severe brain injuries. *Bull. Hosp Joint Dis.* **25**, 170–175 (1964).
4. Giannoudis, P.V., et al. Accelerated bone healing and excessive callus formation in patients with femoral fracture and head injury. *Injury*. **37** Suppl **3**, 18–24 (2006). Erratum in: *Injury*. **38(10)**, 1224 (2007).
5. Locher, R. J. et al. Traumatic brain injury and bone healing: radiographic and biomechanical analyses of bone formation and stability in a combined murine trauma model. *J. Musculoskelet. Neuronal. Interact.* **15**(4), 309–315 (2015).
6. Yang, C. et al. The effect of traumatic brain injury on bone healing from a novel exosome centered perspective in a mice model. *J. Orthop. Translat.* **30**, 70–81 (2021).
7. Song, Y. et al. Increased levels of calcitonin gene-related peptide in serum accelerate fracture healing following traumatic brain injury. *Mol. Med. Rep.* **5**(2), 432–438 (2012).
8. Boes, M., et al. Osteogenic effects of traumatic brain injury on experimental fracture-healing. *J. Bone Joint Surg. Am*. **88(4)**, 738–43 (2006), Erratum in: *J. Bone Joint Surg. Am*. **88(7)**, 1602 (2006).
9. Cadosch, D. et al. Functional and proteomic analysis of serum and cerebrospinal fluid derived from patients with traumatic brain injury: A pilot study. *ANZ J. Surg.* **80**(7–8), 542–547 (2010).
10. Gautschi, O. P. et al. Serum-mediated osteogenic effect in traumatic brain-injured patients. *ANZ J. Surg.* **79**(6), 449–455 (2009).
11. Liu, X. et al. SDF-1 promotes endochondral bone repair during fracture healing at the traumatic brain injury condition. *PLoS ONE* **8**(1), e54077. https://doi.org/10.1371/journal.pone.0054077 (2013).
12. Hackl, M., Heilmeier, U., Weilner, S. & Grillari, J. Circulating microRNAs as novel biomarkers for bone diseases—Complex signatures for multifactorial diseases?. *Mol. Cell Endocrinol.* **432**, 83–95 (2016).
13. Grillari, J. et al. Circulating miRNAs in bone health and disease. *Bone* **145**, 115787. https://doi.org/10.1016/j.bone.2020.115787 (2021).
14. Bartel, D. P. MicroRNAs: Genomics, biogenesis, mechanism, and function. *Cell* **116**(2), 281–297 (2004).
15. Breulmann, F. L. et al. Prognostic and therapeutic potential of microRNAs for fracture healing processes and non-union fractures: A systematic review. *Clin. Transl. Med.* **13**(1), e1161. https://doi.org/10.1002/ctm2.1161 (2023).
16. Komatsu, D. E., Duque, E. & Hadjiargyrou, M. MicroRNAs and fracture healing: Pre-clinical studies. *Bone* **143**, 115758. https://doi.org/10.1016/j.bone.2020.115758 (2021).
17. Groven, R. V. M. et al. Specific microRNAs are associated with fracture healing phases, patient age and multi-trauma. *J. Orthop. Translat.* **37**, 1–11 (2022).
18. Zhao, G., Fu, Y., Yang, C., Yang, X. & Hu, X. Exploring the pathogenesis linking traumatic brain injury and epilepsy *via* bioinformatic analyses. *Front. Aging Neurosci.* **14**, 1047908. https://doi.org/10.3389/fnagi.2022.1047908 (2022).
19. Mitra, B. et al. Plasma micro-RNA biomarkers for diagnosis and prognosis after traumatic brain injury: A pilot study. *J. Clin. Neurosci.* **38**, 37–42 (2017).
20. Pan, Y. B., Sun, Z. L. & Feng, D. F. The role of MicroRNA in traumatic brain injury. *Neuroscience* **367**, 189–199 (2017).
21. Weinberg-Shukron, A., Youngson, N. A., Ferguson-Smith, A. C. & Edwards, C. A. Epigenetic control and genomic imprinting dynamics of the Dlk1-Dio3 domain. *Front. Cell Dev. Biol.* **11**, 1328806. https://doi.org/10.3389/fcell.2023.1328806 (2023).

22. Benetatos, L. et al. The microRNAs within the DLK1-DIO3 genomic region: Involvement in disease pathogenesis. *Cell Mol. Life Sci.* **70**(5), 795–814 (2013).
23. Takegahara, N., Kim, H. & Choi, Y. RANKL biology. *Bone* **159**, 116353. https://doi.org/10.1016/j.bone.2022.116353 (2022).
24. Teasdale, G. & Jennett, B. Assessment of coma and impaired consciousness. A practical scale. *Lancet* **2**(7872), 81–84 (1974).
25. Andermahr, J. et al. Reduced collagen degradation in polytraumas with traumatic brain injury causes enhanced osteogenesis. *J Neurotrauma.* **23**(5), 708–720 (2006).
26. Keller, A. et al. miRNATissueAtlas2: An update to the human miRNA tissue atlas. *Nucl. Acids Res.* **50**(D1), D211–D221 (2022).
27. Agarwal, V., Bell, G. W., Nam, J. W. & Bartel, D. P. Predicting effective microRNA target sites in mammalian mRNAs. *Elife* **4**, e05005. https://doi.org/10.7554/elife.05005 (2015).
28. Hadjiargyrou, M., Salichos, L. & Kloen, P. Identification of the miRNAome in human fracture callus and nonunion tissues. *J. Orthop. Translat.* **39**, 113–123 (2023).
29. Della Bella, E. et al. Identification of circulating miRNAs as fracture-related biomarkers. *PLoS ONE* **19**(5), e0303035. https://doi.org/10.1371/journal.pone.0303035 (2024).
30. Di Pietro, V. et al. MicroRNAs as novel biomarkers for the diagnosis and prognosis of mild and severe traumatic brain injury. *J. Neurotrauma.* **34**(11), 1948–1956 (2017).
31. Redell, J. B., Liu, Y. & Dash, P. K. Traumatic brain injury alters expression of hippocampal microRNAs: Potential regulators of multiple pathophysiological processes. *J. Neurosci. Res.* **87**(6), 1435–1448 (2009).
32. Redell, J. B., Zhao, J. & Dash, P. K. Altered expression of miRNA-21 and its targets in the hippocampus after traumatic brain injury. *J. Neurosci. Res.* **89**(2), 212–221 (2011).
33. Puhakka, N., Das Gupta, S., Vuokila, N. & Pitkänen, A. Transfer RNA-derived fragments and isomiRs are novel components of chronic TBI-induced neuropathology. *Biomedicines.* **10**(1), 136 (2022).
34. Yu, J. et al. Characterization of the lncRNA-miRNA-mRNA regulatory network to reveal potential functional competing endogenous RNAs in traumatic brain injury. *Front. Neurosci.* **16**, 1089857. https://doi.org/10.3389/fnins.2022.1089857 (2023).
35. Du, M. et al. A novel circular RNA, circIgfbp2, links neural plasticity and anxiety through targeting mitochondrial dysfunction and oxidative stress-induced synapse dysfunction after traumatic brain injury. *Mol. Psychiatry.* **27**(11), 4575–4589 (2022).
36. Einhorn, T. A. & Gerstenfeld, L. C. Fracture healing: Mechanisms and interventions. *Nat. Rev. Rheumatol.* **11**(1), 45–54 (2015).
37. Gerstenfeld, L. C. et al. Comparison of effects of the bisphosphonate alendronate versus the RANKL inhibitor denosumab on murine fracture healing. *J. Bone Miner. Res.* **24**(2), 196–208 (2009).
38. Wildburger, R. et al. Post-traumatic hormonal disturbances: Prolactin as a link between head injury and enhanced osteogenesis. *J. Endocrinol. Invest.* **21**(2), 78–86 (1998).
39. World Medical Association. World Medical Association Declaration of Helsinki: Ethical principles for medical research involving human subjects. *JAMA* **310**(20), 2191–2194 (2013).
40. Livak, K. J. & Schmittgen, T. D. Analysis of relative gene expression data using real-time quantitative PCR and the 2(-Delta Delta C(T)) Method. *Methods* **25**(4), 402–408 (2001).

Acknowledgements

We would like to thank the team at TAmiRNA for their valuable support and expertise in conducting the miRNA profiling analyses. We are also deeply grateful to the patients who generously provided their consent and donated blood samples, making this study possible.

Author contributions

A.T., F.W. conceived and designed this study. T.L., F.D., R.G., A.D., V.W., C.D. obtained the data. T.L., F.D., V.H., C.D., M.H., A.T., and F.W. analyzed the data. T.L., F.D., R.G., C.D., A.D., and V.H. performed the experiments. T.L., F.D., C.D., A.D., and V.H. prepared figures. T.L., C.D., and V.H. drafted the manuscript. A.T. and F.W. revised the manuscript. All authors contributed to the article and approved the submitted version.

Funding

Lorenz Böhler Fonds (Grant #1/18); State of Salzburg WISS 2025 (CONSONANT, Grant # F2200397-KZP; GOOD FIBRATION, Grant # 20102/F2400948-FPR; EXMR, Grant # 20102/F2400949-FPR).

Declarations

Competing interests

The authors declare no competing interests.

Ethics approval and consent to participate

The experimental protocol was established according to the ethical guidelines of the Declaration of Helsinki and was approved by the Ethics Commission for the State of Salzburg and informed consent was obtained for all donors (approval number 415-E/2293/4-2018).

Additional information

Supplementary Information The online version contains supplementary material available at https://doi.org/10.1038/s41598-025-27270-9.

Correspondence and requests for materials should be addressed to A.T.